ISSN 1070-3284, Russian Journal of Coordination Chemistry, 2018, Vol. 44, No. 2, pp. 109–116. © Pleiades Publishing, Ltd., 2018.
Original Russian Text © N.V. Somov, F.F. Chausov, R.M. Zakirova, N.V. Lomova, F.Z. Gil'mutdinov, I.N. Shabanova, V.G. Petrov, M.A. Shumilova, D.K. Zhirov, 2018, published in Koordinatsionnaya Khimiya, 2018, Vol. 44, No. 1, pp. 20–27.

Dihydronitrilotris(methylenephosphonato)dimercury(II)mercury(I) $[(Hg_2^I)Hg^{II}N(CH_2PO_3)_3H_2]$: Synthesis and Structure

N. V. Somov[a], *, F. F. Chausov[b, c], R. M. Zakirova[b], N. V. Lomova[b, c], F. Z. Gil'mutdinov[c], I. N. Shabanova[c], V. G. Petrov[d], M. A. Shumilova[d], and D. K. Zhirov[d]

[a] *Lobachevsky National Research University, Nizhny Novgorod, Russia*
[b] *Udmurt State University, Izhevsk, 426034 Russia*
[c] *Physical and Technical Institute, Ural Branch, Russian Academy of Sciences, Izhevsk, Russia*
[d] *Institute of Mechanics, Ural Branch, Russian Academy of Sciences, Izhevsk, Russia*
**e-mail: somov@phys.unn.ru*

Received July 18, 2017

Abstract—Heterovalent complex $[(Hg_2^I)Hg^{II}N(CH_2PO_3)_3H_2]$ is synthesized by the reaction of mercury amidochloride $Hg^{II}NH_2Cl$ with nitrilotris(methylenephosphonic acid) $N(CH_2PO_3)_3H_6$. The gray crystals with metallic luster are monoclinic and described by the space group $P2_1/c$, $Z = 4$, $a = 8.2988(7)$, $b = 22.3149(15)$, $c = 7.2188(6)$ Å, and $\beta = 115.419(11)°$. The Hg(II) atom is coordinated at vertices of a distorted octahedron, and the Hg_2^I group has the configuration of a strongly distorted trigonal prism. Seven donor centers of the ligand, six of the nine oxygen atoms, and one nitrogen atom are involved in the coordination of the mercury atoms. The crystal packing includes layers formed by the two-dimensional connection of the mercury atoms and ligand molecules linked by the van der Waals forces and weak hydrogen bonds only (CIF file CCDC no. 1559444).

Keywords: heterovalent complex, dimercury(I), mercury(II), nitrilotris(methylenephosphonic acid), bridging ligand, chelate complex, X-ray photoelectron spectroscopy, weak hydrogen bonds

DOI: 10.1134/S1070328418020100

INTRODUCTION

Heterovalent complexes containing ions of one metal in various oxidation states are formed, as a rule, in redox processes. A stable heterovalent complex is formed most probably with the ligand capable of forming the bridging fragment $M^N–L–M^{N+1}$ [1]. The M^N and M^{N+1} centers differed by the valence states N and $N + 1$ are characterized by different populations of the valence sublevel. Therefore, if the bridging fragment is electron-conducting, then the so-called intervalence electron transition is possible determining the characteristic properties of the complex: color, electroconductivity, and catalytic and sorption activities.

Coordination compounds of Hg have unique and often poorly explainable structures. Mercury is characterized by the capability of forming polycations the most abundant of which is dimercury(I) cation $(Hg_2^I)^{2+}$ [2–5]. The formation of these clusters is explained by relativistic effects [6], one of which is a strong interaction of atoms with completely filled electronic shells [7]. This determines the binding of mercury atoms to form clusters and polycations [8–11].

The mercury compounds find use in medicine, veterinary, and agriculture as antitumor, antiviral, antiparasitic, and immunomodulatory drugs [12] and as inhibitors of corrosion and self-discharge of chemical current sources [13]. At the same time, mercury is one of the most dangerous ecotoxicants [14]. The mercury complexes are often less toxic than the mercury salts [15] and, therefore, the study of mercury complexes is urgent.

Organopolyphosphonic acids as ligands are distinguished by wide possibilities of coordination and stereochemical diversity of the formed complexes [16]. Nitrilotris(methylenephosphonic acid) $N(CH_2PO_3)_3H_6$ (NTP) belongs to this class of ligands, and its metal complexes are being raptly studied both abroad [17–19] and in Russia [20–25]. The dimercury(I) complex with NTP, whose structure is a three-dimensional framework containing water molecules, was synthesized and studied [26].

The synthesis, crystal structure, spectral properties, and thermal stability of dihydronitrilotris(methylenephosphonato)dimercury(I)mercury(II) $[(Hg_2^I)Hg^{II}N(CH_2PO_3)_3H_2]$ (**I**) are described in this work.

EXPERIMENTAL

Synthesis of complex I. Mercury(II) chloride (analytical grade), ammonia (analytical grade), and doubly recrystallized NTP (the PO_4^{3-} content was not more than 0.3%) were used. Mercury amidochloride $Hg^{II}NH_2Cl$ (infusible white precipitate) was obtained using a described procedure [27, 28]. A stoichiometric excess of an aqueous solution of NTP was poured to mercury amidochloride, and the mixture was left in a corked bottle. In 2 years, gray crystals with metallic luster of complex **I** as needle-like prisms up to 1 mm long were formed in the bottle. The product was mechanically separated, washed consequently with ethanol and diethyl ether, and dried at room temperature.

X-ray diffraction analysis. The crystallographic characteristics and experimental and structure refinement parameters for compound **I** are presented in Table 1. The primary fragment of the structure of complex **I** was determined by a direct method. The positions of non-hydrogen atoms were determined from the electron density difference syntheses and refined in the anisotropic approximation by least squares for $|F|^2$. The positions of hydrogen atoms were determined geometrically. Selected interatomic distances and bond angles in the structure of complex **I** are given in Table 2. The geometric parameters for the crystal structure of compound **I** are presented in Table 3.

The X-ray diffraction results for the structure of complex **I** were deposited with the Cambridge Crystallographic Data Centre (CIF file CCDC no. 1559444; deposit@ccdc.cam.ac.uk or http://www. ccdc.cam.ac.uk/data_request/cif).

The IR absorption spectra of compound **I** were recorded on an FSM-1202 FT-IR spectrometer in a range of 450–5000 cm^{-1} as pellets pressed with KBr.

The Raman spectra of a single crystal of compound **I** were detected in a range of 475–570 nm on a Centaur U-HR microscope/microspectrometer using laser excitation with the wavelength at 473 nm.

The X-ray photoelectron spectrum of compound **I** was recorded on a SPECS spectrometer with a Phoibos-150 semispherical electrostatic energy analyzer (Deutschland) using excitation with the MgK_α radiation ($h\nu$ = 1253.6 eV). The instrument was calibrated by the spectrum of gold (99.9%), and the full width at half maximum (FWHM) of each component of the doublet Au4*f* was 1.2 eV. A sample of compound **I** in the form of fine crystals was deposited on an indium (99.9%) support. The spectra of the Hg4*f*, P2*p*, N1*s*, and O1*s* core levels were recorded. The energy bond (E_B) scale was calibrated by the Na1*s* (64.0), Cl2*p* (198.5), C1*s* (285.0), and In3*d* (443.5 eV) lines taking into account the linear regression correction relative to E_B. The background and inelastic scattering were taken into account according to Shirley [34].

The thermogravimetric analysis of compound **I** was conducted on a Shimadzu DTG-60H automated derivatograph in an Ar atmosphere in a range of 30–500°C at a heating rate of 3°C/min.

RESULTS AND DISCUSSION

The asymmetric formula unit of complex **I** (Fig. 1) is described by the point group of the C_1 symmetry. The ligand molecule undergoes a considerable deformation upon complex formation. The bond angles at the nitrogen atoms have a substantial scatter, but the average value (109.5(20)°) is well consistent with the ideal tetrahedral angle. The N–C (1.479(10)–1.517(9) Å) and C–P (1.790(7)–1.832(7) Å) distances vary significantly. The NTP molecule is fourfold protonated and retains two protons localized on the O(3) and O(4) atoms involved in hydrogen bonds. All other oxygen atoms coordinate the mercury atoms. The denticity of the ligand is 8 with allowance for the nitrogen atom.

The Hg(2) atom is coordinated at the vertices of the distorted octahedron by the nitrogen atom and five oxygen atoms. The Hg(2)–N(1) distance (2.185(6) Å) is closer to the sum of covalent radii (r_C(N) = 0.71 Å [35, 36], r_C(Hg) = 1.32 Å [35] or 1.33 Å [36]) than to the sum of ionic radii (r_I(N) = 1.46 Å, r_I(Hg) = 1.02 Å [37]). The Hg(2)–O distances show a significant scatter (2.084(6)–2.858(5) Å). The average value (2.52(26) Å) considerably exceeds the sum of covalent radii (r_C(O) = 0.66 Å [35] or 0.63 Å [36]) and is substantially higher than the sum of ionic radii (r_I(O) = 1.36 Å [37]). It is most likely that the observed distortion appeared as a difference in bond lengths of the coordination polyhedron of Hg(2) is caused by significant mechanical stresses during the formation of the crystal packing of complex **I**, whereas an increase in the average Hg(2)–O distance compared to the sum of atomic radii is explained by the Urusov distortion theorem [38, 39]. For the coordination of the Hg(2) atom, the NTP ligand exhibits the chelate function closing three intramolecular rings N–Hg–O–P–C with the common N–Hg bond.

The Hg(1) and Hg(3) atoms compose the dumbbell-like $(Hg_2^I)^{2+}$ dimercury ions with the Hg(3)^i and Hg(1)^{ii} atoms, respectively, of the adjacent structural units. The coordination polyhedron of the dimercury ion is a distorted trigonal prism, whose vertices are occupied by six oxygen atoms. The Hg–O distances in the environment of the dimercury ion have a significant scatter (2.149(5)–2.756(5) Å (average 2.42(19) Å)). The scatter of the Hg–O distances in the environment of the $(Hg_2^I)^{2+}$ ion was also mentioned [40], but no correlation of the Hg–O distances with any crystallochemical parameters was found. It has been mentioned [2–4] that the Hg–O dis-

Table 1. Crystallographic data and the experimental and structure refinement data

Parameter	Value
Empirical formula	$[(Hg_2^I)Hg^{II}N(CH_2PO_3)_3H_2]$
FW	896.78
Crystal system; *Z*	Monoclinic; 4
Space group	$P2_1/c$
Cell parameters:	
a, Å	8.2988(7)
b, Å	22.3149(15)
c, Å	7.2188(6)
β, deg	115.419(11)
V, Å^3	1207.41(19)
ρ_{calc}, g/cm^3	4.933
Radiation; λ, Å; monochromator	MoK_α; 0.71073; graphite
μ, mm^{-1}	38.489
T, K	293(2)
Crystal sizes, mm	0.131 × 0.093 × 0.030
Diffractometer	Xcalibur, Sapphire3, Gemini
Scan mode	ω
Absorption correction, T_{min}/T_{max}	Analytically [29], 0.041/0.344
$\theta_{min}/\theta_{max}$, deg	3.27–26.371
Ranges *h*, *k*, *l*	$-10 \le h \le 10$, $-27 \le k \le 27$, $-9 \le l \le 9$
Number of measured/independent reflections (N_1)	16801/2457
R_{Int}	0.0956
Number of reflections with $I > 2\sigma(I)$ (N_2)	2248
Refinement procedure	Full-matrix least squares for F^2
Number of parameters/constraints	160/30
GOOF	1.127
R_1/wR_2 for N_1	0.0402/0.0765
R_1/wR_2 for N_2	0.0358/0.0747
$\Delta\rho_{min}/\Delta\rho_{max}$, *e*/Å^3	−2.009/2.495
Programs	CrysAlisPro [30], SHELX [31], WinGX [32], VESTA 3.0 [33]

tance tends to increasing with a decrease in the HgHgO angle, i.e., with the deviation of the oxygen atom from the axial position of the "dumbbell." The plot of the linear regression of the Hg–O distance vs. HgHgO angle in complex **I** is shown in Fig. 2. It can be seen that a very tight negative correlation is observed, and in the limit at ∠HgHgO → 180° the Hg–O distance tends to the sum of the covalent radii of mercury and oxygen (1.96–1.98 Å).

Unlike the crystal packing in the earlier studied dimercury(I) complex with NTP (three-dimensional framework) [26], the crystal packing of complex **I** presented in Fig. 3 is layered. The layers are formed by formula units symmetric relative to the sliding reflection planes (040). The formula units are linked in the layers by strong covalent Hg–Hg bonds and coordination Hg–O bonds.

The layers are symmetric relative to the inversion center and are linked by the van der Waals forces and weak hydrogen bonds C–H···O (Fig. 3a). The possibility of hydrogen bonding involving the C–H groups, in particular, in crystals, has been described long ago [41, 42]. The role of these bonds in the formation of the crystal structure is actively discussed [43–45]. The structure of compound **I** is an example of a crystal with pronounced heterodesmicity in which the 2D layers of the coordination polymer formed by covalent and coordination bonds are linked by weak interactions only. It is most likely that the possibility of the stable

Table 2. Selected interatomic distances (*d*) and bond angles (ω) in the structure of $[(Hg_2^I)Hg^{II}N(CH_2PO_3)_3H_2]$*

Bond	*d*, Å	Bond	*d*, Å	Bond	*d*, Å
N(1)–C(1)	1.479(10)	P(2)–O(5)	1.519(6)	Hg(2)–O(2)	2.659(5)
N(1)–C(2)	1.517(9)	P(2)–O(6)	1.518(5)	Hg(2)–O(5)	2.408(4)
N(1)–C(3)	1.513(8)	P(3)–O(7)	1.507(5)	Hg(2)–O(8)	2.594(5)
C(1)–P(1)	1.832(7)	P(3)–O(8)	1.519(5)	Hg(2)–O(9)	2.858(5)
C(2)–P(2)	1.790(7)	P(3)–O(9)	1.547(6)	Hg(2)–O(9)#	2.084(6)
C(3)–P(3)	1.813(8)	Hg(1)–Hg(3)	2.5062(5)	Hg(3)–O(2)	2.756(5)
P(1)–O(1)	1.492(5)	Hg(1)–O(2)	2.447(5)	Hg(3)–O(5)	2.436(5)
P(1)–O(2)	1.530(6)	Hg(1)–O(6)	2.470(6)	Hg(3)–O(7)	2.149(5)
$P(1)–O(3)^H$	1.552(6)	Hg(1)–O(8)	2.249(5)		
$P(2)–O(4)^H$	1.553(6)	Hg(2)–N(1)	2.185(6)		
Angle	ω, deg	Angle	ω, deg	Angle	ω, deg
C(1)N(1)C(2)	108.4(6)	O(5)P(2)C(2)	105.9(3)	Hg(3)Hg(1)O(8)	153.59(13)
C(1)N(1)C(3)	112.0(5)	O(6)P(2)C(2)	106.7(3)	$N(1)Hg(2)O(9)^{\#}$	177.08(19)
C(2)N(1)C(3)	108.7(5)	$O(4)^HP(2)O(5)$	112.7(3)	O(8)Hg(2)O(9)	162.83(10)
C(1) N(1)Hg(2)	106.1(4)	$O(4)^HP(2)O(6)$	111.2(3)	O(2)Hg(2)O(5)	138.97(13)
C(2) N(1)Hg(2)	110.8(4)	O(5)P(2)O(6)	113.5(3)	N(1)Hg(2)O(2)	77.02(13)
C(3) N(1)Hg(2)	110.9(4)	O(7)P(3)C(3)	108.8(3)	N(1)Hg(2)O(5)	82.40(14)
N(1)C(1)P(1)	114.4(5)	O(8)P(3)C(3)	105.6(3)	N(1)Hg(2)O(8)	102.62(14)
N(1)C(2)P(2)	115.8(5)	O(9)P(3)C(3)	104.7(3)	N(1)Hg(2)O(9)	78.64(14)
N(1)C(3)P(3)	116.3(5)	O(7)P(3)O(8)	115.1(3)	O(2)Hg(2)O(8)	68.38(12)
O(1)P(1)C(1)	107.6(3)	O(7)P(3)O(9)	111.4(3)	O(2)Hg(2)O(9)	95.60(11)
O(2)P(1)C(1)	107.7(3)	O(8)P(3)O(9)	110.5(3)	O(5)Hg(2)O(8)	82.31(12)
$O(3)^HP(1)C(1)$	104.6(3)	Hg(1)Hg(3)O(2)	93.73(8)	O(5)Hg(2)O(9)	114.72(11)
O(1)P(1)O(2)	116.3(3)	Hg(1)Hg(3)O(5)	117.13(13)	$O(9)^{\#}Hg(2)O(2)$	102.72(12)
$O(1)P(1)O(3)^H$	108.3(3)	Hg(1)Hg(3)O(7)	158.77(14)	$O(9)^{\#}Hg(2)O(5)$	99.51(14)
$O(2)P(1)O(3)^H$	111.7(3)	Hg(3)Hg(1)O(2)	124.15(11)	$O(9)^{\#}Hg(2)O(8)$	79.92(14)
$O(4)^HP(2)C(2)$	106.2(3)	Hg(3)Hg(1)O(6)	109.76(12)	$O(9)^{\#}Hg(2)O(9)$	98.49(14)

* $O(3)^H$ and $O(4)^H$ are protonated oxygen atoms; # designates the symmetrically equivalent position: $x, -y + 1/2, z + 1/2$.

Table 3. Geometric parameters of hydrogen bonds in the crystal packing of $[(Hg_2^I)Hg^{II}N(CH_2PO_3)_3H_2]$*

D–H···A	Distance, Å			Angle D–H···A, deg
	D–H	H···A	D···A	
$O(3)–H(3)···O(6)^{iii}$	0.85(3)	1.91(3)	2.7055(2)	156(3)
$O(4)–H(4)···O(1)^{iv}$	0.83(3)	1.90(3)	2.713(2)	169(3)
$C(1)–H(1A)···O(1)^{i}$	0.80(3)	2.02(3)	2.822(2)	174(3)
C(1)–H(1*B*)···O(4)	0.77(3)	1.98(3)	2.743(2)	172(3)
$C(2)–H(2A)···O(4)^{ii}$	0.81(3)	2.32(3)	3.096(2)	161(3)
C(2)–H(2*B*)···O(7)	0.74(3)	2.00(3)	2.724(2)	169(3)
$C(3)–H(3A)···O(1)^{i}$	0.79(3)	1.95(3)	2.732(2)	177(3)
$C(3)–H(3B)···O(6)^{iii}$	0.74(3)	1.95(3)	2.694(2)	175(3)

Symmetrically equivalent positions: i $-x, -y, -z$; ii $-x + 1, -y, -z$; iii $x - 1, y, z$; iv $x + 1, -y - 1/2, z$.

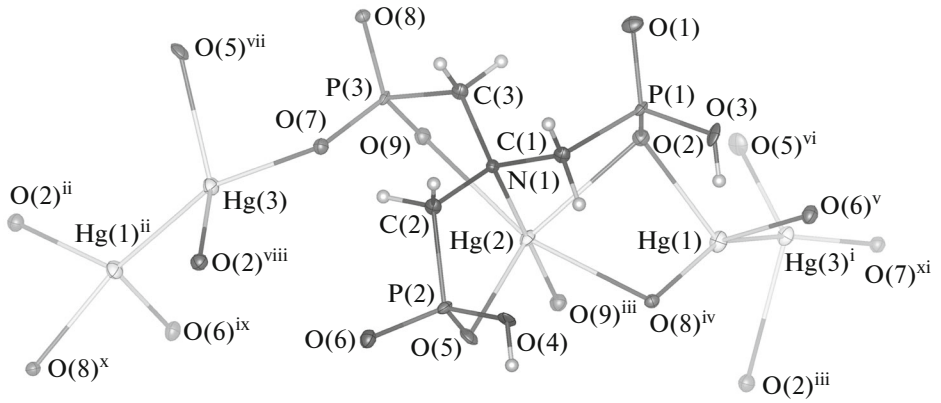

Fig. 1. Structural unit of compound **I**. Symmetrically equivalent positions: [i] $x + 1, -y - 1/2, z - 1/2$; [ii] $x - 1, -y - 1/2, z + 1/2$; [iii] $x, -y - 1/2, z - 1/2$; [iv] $x, y, z - 1$; [v] $x + 1, y, z$; [vi] $x + 1, -y - 1/2, z + 1/2$; [vii] $x, y, z + 1$; [viii] $x - 1, y, z$; [ix] $x, -y - 1/2, z + 1/2$; [x] $x - 1, -y - 1/2, z - 1/2$; [xi] $x + 1, -y - 1/2, z - 1/2$.

existence for this structure is caused by a high degree of geometric correspondence of the positions of the C–H groups and the acceptor O atoms in the adjacent layers, due to which the formed interlayer C–H···O bonds in the structure of compound **I** (H···O 1.95(3)–2.32(3), C–O 2.733(2)–3.096(2) Å) are significantly shorter than the C–H···O bonds in the most part of the previously described compounds [44].

Each layer represents a continuous two-dimensional bonding formed by the mercury cations in different oxidation states linked by the bridging oxygen atoms (Fig. 3b). The Hg^{2+} ion in the Hg(2) position is linked with the adjacent Hg^{2+} ion by the O(9) atom and also by the Hg(1) and Hg(3) atoms of the $(Hg_2^I)^{2+}$ ions via the O(2) and O(7) atoms, respectively. Owing to this, there is a possibility of the intervalence electron transition in complex **I**.

The molecular vibration spectra (Fig. 4) confirm the described structure of compound **I**. The band at 176 cm^{-1} is assigned to the ν(Hg–Hg) vibrations [46, 47]. The triplet at 460, 485, and 503 cm^{-1} assigned to the ν(Hg–O) vibrations corresponds to the broad band in the Raman spectrum with a maximum at 464 cm^{-1}. The band at 575 cm^{-1}, which is intense in both spectra, corresponds to ν(Hg–N), which is consistent with published data [48, 49]. The nonequivalence of all CH_2PO_3 branches of the NTP molecule is manifested as numerous bands of deformation vibrations of the N–C–P skeleton in a range of 670–900 cm^{-1}. The group of intense bands in a range of 950–1190 cm^{-1} is assigned to vibrations of three symmetrically nonequivalent PO_3 groups. The vibrations of the partially localized π-P–O bonds are manifested as a group of bands at 1220–1275 cm^{-1}. As a whole, the vibrations of the ligand skeleton do not obey the alternative prohibition rule, which indicates the asymmetric conformation of the NTP molecule. The doublets δ_{as}–$\delta_s(CH_2)$ at 1406–1409 cm^{-1} and ν_{as}–$\nu_s(CH_2)$ in a range of 2900–2990 cm^{-1} are split into three components each indicating that all CH_2 groups are nonequivalent.

The fragment of the X-ray photoelectron spectrum of compound **I** including the $Hg4f_{7/2-5/2}$ doublet is shown in Fig. 5. The significant width and asymmetry of the components of the doublet are observed indicating that the mercury atoms in compound **I** are nonequivalent. The approximation of the spectrum by the Voigt functions with an FWHM of 1.2 eV was performed using the Fityk 0.9.8 program [50]. The

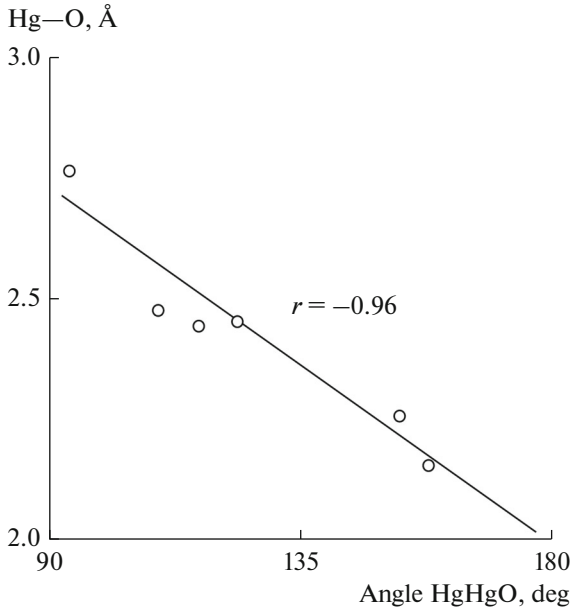

Fig. 2. Correlation of the Hg–O distance with the HgHgO angle in the coordination environment of the dimercury(I) ion.

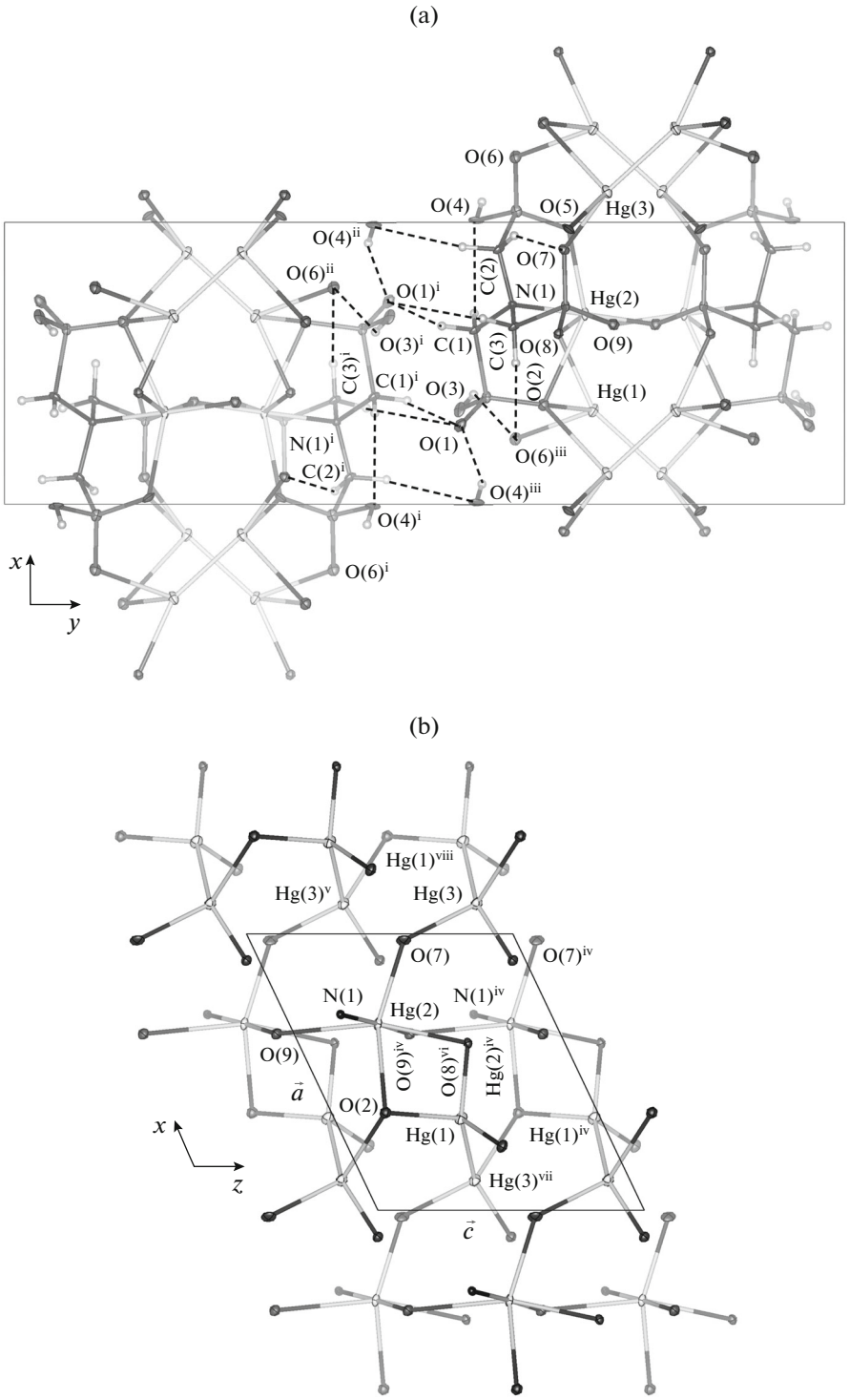

Fig. 3. Crystal packing of compound **I**: (a) the layered structure in the projection along the *c* axis and (b) the two-dimensional Hg–O bond of one layer of the packing in the projection onto the (010) plane. Symmetrically equivalent positions: [i] $-x, -y, -z$; [ii] $-x+1, -y, -z$; [iii] $x-1, y, z$; [iv] $x, -y-1/2, z+1/2$; [v] $x+1, -y-1/2, z$; [vi] $x, y, z+1$; [vi] $x-1, -y-1/2, z-1/2$; [viii] $x+1, -y-1/2, z+1/2$.

best agreement is achieved for the approximation by curves *2* and *3* with the ratio of integral intensities 2 : 1. It can be concluded that the more intense components of the doublet Hg4$f_{7/2-5/2}$ with $E_B = 100.2$ and 104.7 eV are attributed to the Hg(1) and Hg(3) atoms, whereas the components with $E_B = 100.7$ and 105.2 eV

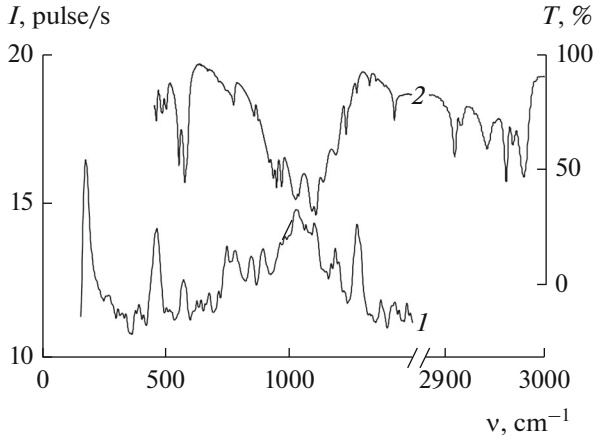

Fig. 4. (*1*) Raman and (*2*) IR spectra of complex **I** (intensity I and transmittance T as functions of the wave number ν).

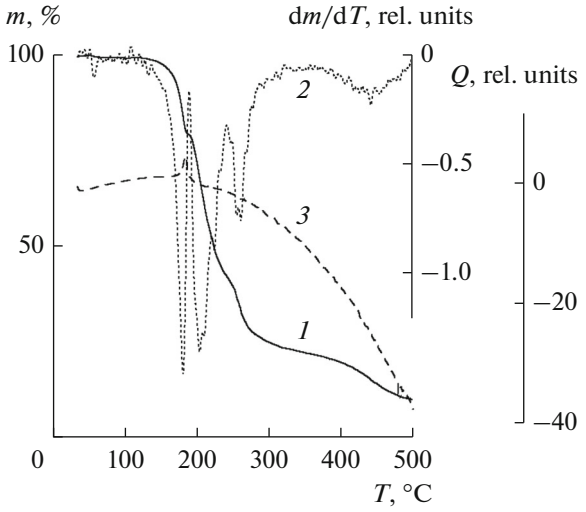

Fig. 6. Thermograms of complex **I** in an argon atmosphere: (*1*) the weight m, (*2*) derivative dm/dT, and (*3*) heat release Q (*3*) as functions of temperature T.

are assigned to the Hg(2) atom. Thus, the mercury atoms in complex **I** are in the nonequivalent redox states.

The thermogravimetric study of HgNTP (Fig. 6) showed a sharp distinction of the thermochemical behavior of complex **I** from that of the earlier studied complex [26]. The absence of water molecules in the structure of compound **I** results in the absence of noticeable changes below 150°C. The exothermic effect with the loss of one mercury atom is observed in a range of 150–190°C, most likely, due to the disproportionation of the $(Hg_2^I)^{2+}$ cation to Hg^{2+} and Hg^0. A significant mass loss (corresponding to $M_r \approx 322$) occurs at 190–242°C and is caused by the elimination of the second mercury atom and, probably, the fragment of the organic skeleton of the ligand molecule. After this, the run of the base line of the temperature effect curve changes, most likely, due to the melting of the decomposition products. The third mercury atom is lost in a range of 242–300°C. The further mass loss is observed above 380°C due to the evaporation of the thermal decomposition products.

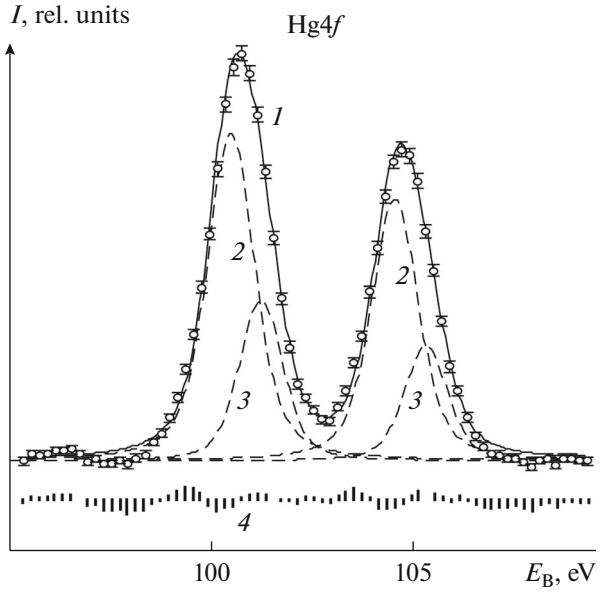

Fig. 5. X-ray photoelectron spectrum of complex **I** (intensity I as a function of the bond energy E_B): (*1*) experimental points with 95% confidence intervals, contributions from the (*2*) $(Hg_2^I)^{2+}$ and (*3*) Hg^{2+} ions, and (*4*) decoupling with experimental data.

ACKNOWLEDGMENTS

This work was carried out in the framework of the basic part of the state task for higher educational institutions and scientific organizations in the sphere of scientific activities (project no. 3.6502.2017/BCh).

REFERENCES

1. Avdeeva, V.V., Dziova, A.E., Polyakova, I.N., et al., *Dokl. Chem.*, 2011, vol. 437, p. 79.
2. Magarill, S.A., Pervukhina, N.V., Borisov, S.V., and Pal'chik, N.A., *Kristallokhimiya soedinenii nizkovalentnoi rtuti* (Crystal Chemistry of Low-Valent Mercury Compounds), Moscow: Yanus-K, 2001.
3. Pervukhina, N.V., Romanenko, G.V., Borisov, S.V., et al., *J. Struct. Chem.*, 1999, vol. 40, p. 461.
4. Pervukhina, N.V., Magarill, S.A., Borisov, S.V., et al., *Russ. Chem. Rev.*, 1999, vol. 68, no. 8, p. 615.
5. Borisov, S.V., Magarill, S.A., Romanenko, G.V., and Pervukhina, N.V., *J. Struct. Chem.*, 2000, vol. 41, p. 272.
6. Pyykkö, P., *Chem. Rev.*, 1988, vol. 88, p. 563.
7. Pyykkö, P., *Chem. Rev.*, 1997, vol. 97, p. 597.

8. Kaupp, M. and von Schnering, H.G., *Inorg. Chem.*, 1994, vol. 33, no. 12, p. 2555.
9. Kaupp, M. and von Schnering, H.G., *Inorg. Chem.*, 1994, vol. 33, no. 18, p. 4179.
10. Volkova, L.M. and Magarill, S.A., *J. Struct. Chem.*, 1999, vol. 40, p. 262.
11. Duval, M.-C., Soep, B., and Breckenridge, W.H., *J. Phys. Chem.*, 1991, vol. 95, p. 7145.
12. Gusev, S.N., Gusev, R.S., and Gramma, A.I., RF Patent 2456001, 2012, p. 24.
13. Romanov, V.V. and Khashev, Yu.M., *Khimicheskie istochniki toka* (Chemical Current Sources), Moscow: Sovetskoe radio, 1968.
14. Petrosyan, V.S., *Ekologiya i promyshlennost' Rossii*, 1999, no. 12, p. 34.
15. Swaran, J.S.F. and Vidhu, P., *Int. J. Environ. Res. Public Health*, 2010, vol. 7, no. 7, p. 2745.
16. Dyatlova, N.M., Temkina, V.Ya., and Popov, K.I., *Kompleksony i kompleksonaty metallov* (Complexones and Metal Complexonates), Moscow: Khimiya, 1988.
17. Cabeza, A., Ouyang, X., Sharma, C.V.K., et al., *Inorg. Chem.*, 2002, vol. 41, p. 2325.
18. Demadis, K.D., Katarachia, S.D., and Koutmos, M., *Inorg. Chem. Commun.*, 2005, vol. 8, p. 254.
19. Bazaga-Garcia, M., Angeli, G.K., Papathanasiou, K.E., et al., *Inorg. Chem.*, 2016, vol. 55, no. 15, p. 7414.
20. Somov, N.V. and Chausov, F.F., *Cryst. Rep.*, 2014, vol. 59, no. 1, p. 66.
21. Somov, N.V. and Chausov, F.F., *Cryst. Rep.*, 2015, vol. 60, no. 2, p. 210.
22. Somov, N.V., Chausov, F.F., Zakirova, R.M., et al. *Cryst. Rep.*, 2015, vol. 60, no. 6, p. 853.
23. Somov, N.V., Chausov, F.F., Zakirova, R.M., and Fedotova, I.V., *Cryst. Rep.*, 2016, vol. 61, no. 2, p. 216.
24. Somov, N.V., Chausov, F.F., Zakirova, R.M., and Fedotova, I.V., *Russ. J. Coord. Chem.*, 2015, vol. 41, no. 12, p. 798.
25. Somov, N.V., Chausov, F.F., and Zakirova, R.M., *Cryst. Rep.*, 2016, vol. 61, no. 4, p. 606.
26. Somov, N.V., Chausov, F.F., Zakirova, R.M., et al., *Russ. J. Coord. Chem.*, 2016, vol. 42, no. 1, p. 37.
27. Sen, J., *Z. Anorg. Allg. Chem.*, 1903, vol. 33, p. 197.
28. Lipscomb, W.N., *Acta Crystallogr.*, 1951, vol. 4, p. 266.
29. Clark, R.C. and Reid, J.S., *Acta Crystallogr., Sect. A: Found. Cryst.*, 1995, vol. 51, p. 887.
30. Rigaku, *CrysAlis PRO,* Rigaku Oxford Diffraction, Yarnton, Oxfordshire, 2016.
31. Sheldrick, G.M., *Acta Crystallogr., Sect. A: Found. Crystallogr.*, 2008, vol. 64, p. 112.
32. Farrugia, L.J., *J. Appl. Crystallogr.*, 1999, vol. 32, p. 837.
33. Momma, K. and Izumi, F., *J. Appl. Crystallogr.*, 2011, vol. 44, p. 1272.
34. Shirley, D.A., *Phys. Rev.*, 1972, vol. 55, p. 4709.
35. Cordero, B., Gömez, V., Platero-Prats, A.E., et al., *Dalton Trans.*, 2008, no. 21, p. 2832.
36. Pyykkö, P. and Atsumi, M., *Chem.-Eur. J.*, 2009, vol. 15, p. 186.
37. Shannon, R.D., *Acta Crystallogr., Sect. A: Cryst. Phys., Diffr., Theor. Gen. Crystallogr.*, 1976, vol. 32, p. 751.
38. Urusov, V.S., *Acta Crystallogr., Sect. B: Struct. Crystallogr. Cryst. Chem.*, 1995, vol. 51, p. 641.
39. Urusov, V.S., *Z. Kristallogr.*, 2003, vol. 218, p. 709.
40. Lundberg, D. and Persson, I., *Z. Kristallogr.*, 2012, vol. 227, p. 683.
41. Glasstone, S., *Trans. Faraday Soc.*, 1937, vol. 33, p. 200.
42. Sutor, D.J., *Nature*, 1962, vol. 195, p. 68.
43. Desiraju, G.R., *Acc. Chem. Res.*, 1991, vol. 24, p. 290.
44. Steiner, T., *Crystallogr. Rev.*, vol. 6, p. 1.
45. Grabowski, S.J., *Crystals*, 2016, vol. 6, p. 59.
46. Russell, S.J., Tan, K.-H., and Taylor, M.J., *J. Raman Spectrosc.*, 1980, vol. 9, no. 5, p. 308.
47. Baran, E.J., Mormann, T., and Jeitschko, W., *J. Raman Spectrosc.*, 1999, vol. 30, no. 12, p. 1049.
48. Canty, A.J. and Devereux, J.W., *Spectrochim. Acta, Part A*, 1980, vol. 36, no. 5, p. 495.
49. Rama Krishna Reddy, K., Suneetha, P., Karigar, C.S., et al., *J. Chil. Chem. Soc.*, 2008, vol. 53, no. 4, p. 1653.
50. Wojdyr, M., *J. Appl. Crystallogr.*, 2010, vol. 43, p. 1126.

Translated by E. Yablonskaya